Journal of Membrane Science 493 (2015) 206–211

Contents lists available at ScienceDirect

Journal of Membrane Science

journal homepage: www.elsevier.com/locate/memsci

Preparation of graded silicalite-1 substrates for all-zeolite membranes with excellent CO_2/H_2 separation performance

Farid Akhtar [a,b,*], Erik Sjöberg [c], Danil Korelskiy [c], Mark Rayson [d], Jonas Hedlund [c], Lennart Bergström [a,*]

[a] Department of Materials and Environmental Chemistry, Stockholm University, SE-10691 Stockholm, Sweden
[b] Division of Materials Science, Luleå University of Technology, SE-97187 Luleå, Sweden
[c] Chemical Technology, Luleå University of Technology, SE-97187 Luleå, Sweden
[d] Department of Chemistry, The University of Surrey, Guildford, Surrey GU2 7XH, UK

ARTICLE INFO

Article history:
Received 18 March 2015
Received in revised form
3 June 2015
Accepted 6 June 2015
Available online 23 June 2015

Keywords:
All-zeolite membranes
Membrane separation
Gas separation
Cracking
Thermal cycling

ABSTRACT

Graded silicalite-1 substrates with a high gas permeability and low surface roughness have been produced by pulsed current processing of a thin coating of a submicron silicalite-1 powder onto a powder body of coarser silicalite-1 crystals. Thin zeolite films have been hydrothermally grown onto the graded silicalite-1 support and the all-zeolite membranes display an excellent CO_2/H_2 separation factor of 12 at 0 °C and a CO_2 permeance of 21.3×10^{-7} mol m^{-2} s^{-1} Pa^{-1} for an equimolar CO_2/H_2 feed at 505 kPa and 101 kPa helium sweep gas. Thermal cracking estimates based on calculated surface energies and measured thermal expansion coefficients suggest that all-zeolite membranes with a minimal thermal expansion mismatch between the graded substrate and the zeolite film should remain crack-free during thermal cycling and the critical calcination step.

1. Introduction

Inorganic zeolite membranes consisting of highly crystalline microporous aluminosilicate films supported onto a porous substrate [1–3] have shown promise for energy-efficient production and upgrading of biofuels [4,5], carbon dioxide separation from CO_2/CH_4, CO_2/N_2, and CO_2/H_2 gas mixtures [6–9], and pervaporation [4]. Zeolite membranes have been prepared of a limited number of framework types; FAU [8], DDR [10], LTA [11], MOR [12,13] and MFI [6], where MFI zeolite membranes have gained a large research interest due to a high thermal, chemical and mechanical stability [7,14,15].

The performance of zeolite membranes is primarily controlled by the properties of the zeolite films that should have a well-defined pore size and shape, be as thin as possible to maximize the flux, and be free from macroscopic defects and cracks. The presence of defects and microcracks in the zeolite film is problematic as they greatly reduce the separation performance of the membrane. The zeolite film is usually supported onto a substrate that provides sufficient mechanical strength for handling and thermal or pressure cycling. Commonly used membrane supports for MFI film are α and γ alumina [6,7,16,17], stainless steel [18], clay [19], cordierite [20], glass [21] and carbon [22]. While substrate materials like alumina have a high strength and are relatively easy to manufacture, differences in coefficient of thermal expansion (CTE) between the support and the MFI film may build up thermal stresses during thermal cycling in zeolite film, which could lead to grain boundary openings and cracks. Many zeolites have in fact negative CTE, the CTE of MFI is e.g. $-(1–3) \times 10^{-6}$ °C^{-1} [23], while commonly used alumina substrate alumina have positive CTE; ranging between 8.0 and 8.8×10^{-6} °C^{-1} [24].

Recent advances in zeolite membrane research have shown significant improvements in membrane synthesis and separation performance [7,14]. Important advances have been made to minimize and treat defects and cracks including e.g. tailoring the microstructure during film crystallization [25,26], selective chemical vapour deposition of coke and silica at defects [27,28], and condensation of Si–OH groups by rapid thermal treatment [14]. Although these advances show promise, there is a need to engineer the membranes to minimize the thermally induced stresses.

Thermal cracking of laminated systems can be reduced by either reducing the film thickness or by minimizing or eliminating the difference in the CTE between the zeolite film and membrane support [29,30]. Reducing the zeolite film thickness to tens of nanometres compared to current state-of-the-art zeolite films of

* Corresponding authors at: Department of Materials and Environmental Chemistry, Stockholm University, SE-10691 Stockholm, Sweden. Tel.: +46 81 63568; fax: +46 81 52781.
E-mail addresses: farid.akhtar@mmk.su.se (F. Akhtar), lennart.bergstrom@mmk.su.se (L. Bergström).

http://dx.doi.org/10.1016/j.memsci.2015.06.020

500 nm [25] is difficult using synthesis routes based on seeding followed by hydrothermal growth [15]. In this study, we demonstrate how all-zeolite MFI membranes consisting of an MFI zeolite film grown on a graded MFI zeolite support with a similar CTE and high gas permeability can be produced. The preparation and characterization of the graded MFI support and the CO_2/H_2 separation performance of the all-zeolite membranes are reported.

2. Experimental

2.1. Materials

Silicalite-1 powders (Sud-Chemie AG, Bruckmuhl, Germany) with silica-to-alumina ratios of 1200 and 400 and a particle size of 5 μm were used. Commercially available graded α-alumina supports (Fraunhofer IKTS, Munich, Germany) with a diameter of 25 mm and a thickness of 3 mm thickness were used as reference.

2.2. Processing of graded silicalite-1 membrane supports

The silicalite-1 powder was gently ball milled in deionized water with zirconia balls of 6 mm as milling media in a polymer container to prepare a water-based suspension of fine silicalite-1 particles [31]. Polyethylene glycol (PEG) was added to the aqueous silicalite-1 dispersion to yield dispersions with a solid loading of 10–15 wt% and a PEG content of 3 dwb%. Thin silicalite-1 film with a thickness of 40–60 μm were drop casted from aqueous silicalite-1/PEG dispersions on graphite papers with a diameter of 25 mm. The silicalite-1 coated graphite paper was placed in a cylindrical graphite die and 1.8 g of dry silicalite-1 particles were added. The powder body was pulsed current processed (PCP) in a so called spark plasma sintering machine (Dr. Sinter 2050, Sumitomo Coal Mining Co., Ltd., Japan) The powder assemblies were first heated to a temperature of 600 °C at a heating rate of 200 °C min^{-1} and then heated to 1200 °C at a heating rate of 100 °C min^{-1}. The powder assemblies were kept at 1200 °C for 3 min. The PCP was performed following a procedure described in our previous work on silicalite-1 [24].

2.3. Film growth

Supported silicalite-1 films with a thickness of ca. 0.5 μm were prepared mainly following a method described earlier [25] that is briefly summarized below. Prior to film synthesis, the graded supports were masked [32]. This process involves rinsing of the disks with acetone, followed by covering the wet top surface with PMMA CM205 (Polykemi). After drying, the pores in the graded supports were filled with Sasol wax C-105 (Carbona AB). In order to grow an ultra-thin uniform zeolite film, the masked supports were seeded with a monolayer of colloidal silicalite-1 crystals of ca. 50 nm in size. The film synthesis was carried out hydrothermally at 88 °C for 96 h. The molar composition of the synthesis mixture was $3TPAOH:25SiO_2:1450H_2O:100C_2H_5OH$. After the synthesis, the membranes were rinsed in a 0.1 M solution of ammonia for 24 h and calcined at 500 °C for 6 h. The heating and cooling rates during calcination were 0.2 °C min^{-1} and 0.3 °C min^{-1}, respectively.

2.4. Characterization

The microstructure of the graded membrane supports were characterised on a field emission gun scanning electron microscope (FEG-SEM), JSM-7000F (JEOL, Tokyo, Japan). The biaxial flexural strength of the membrane supports was determined using a cylinder on 3 balls geometry on a Zwick Z050 machine (Zwick GmBH Co & KG, Ulm, Germany). Mercury intrusion porosimetry (MIP) was performed within the pore diameter range of $125\ \mu m \geq \Phi \geq 3$ nm on an Auto Pore III 9410 (Micromeritics, Norcross GA, USA) to determine macropore volume and the pore size distribution. Brunauer, Emmett and Teller (BET) surface area was obtained from nitrogen adsorption and desorption data collected on an ASAP 2020 analyzer (Micromeritics, Norcross GA, USA) within the 0.05–0.15 p/p_o relative pressure region. A degassing of as-received powder or membrane supports was performed prior to nitrogen adsorption at 300 °C for 10 h

Single component permeation of H_2, He and N_2, through the graded zeolite supports and all-zeolite membranes, were measured on a volumetric flow measurement device with a digital output (ADM2000 Flowmeter, Agilent). Prior to measurements, the membrane supports were kept at 300 °C for 6 h for degassing. The pressure of 1 bar was maintained on the permeate side of membrane support and all-zeolite membranes and the applied pressure difference (ΔP) was varied from 0.1 to 1 bar at 25 °C. The CTE of graded silicalite-1 membrane support and alumina supports was measured using a DIL 402 C, horizontal push rod dilatometer (NETZSCH-Geratebau GmBH, Selb, Germany). The CTE measurements were performed on specimens with a length of 24 mm and a square cross-section 3×3 mm. The CTE was determined from 200 °C to 800 °C.

2.5. Gas separation measurements

The gas separation performance of the all-zeolite membranes was evaluated at 0 °C using an equimolar mixture of CO_2 and H_2. The total feed volumetric flow rate was 3 l min^{-1}. The total feed pressure was varied stepwise from 1 to 5 bar whereas the total permeate pressure was atmospheric. All experiments were performed using a 101 kPa helium sweep gas at a volumetric flow rate of 0.75 l min^{-1}. Prior to the separation experiments, the membrane was flushed with helium overnight using feed and permeate volumetric flow rates of 0.3 l min^{-1} at atmospheric pressure in order to desorb moisture. The permeate volumetric flow rate was measured with a drum-type gas meter (TG Series, Ritter Apparatebau GmbH) and the permeate composition was analysed by a mass spectrometer (GAM 400, InProcess Instruments) connected on-line. The permeance of component i (mol s^{-1} m^{-2} Pa^{-1}) was estimated from the measured molar flow of the corresponding component through the membrane F_i (mol s^{-1}) as

$$\Pi_i = F_i/(A\Delta P_i), \tag{1}$$

where A is the membrane area (m^2) and ΔP_i (Pa) is the partial pressure difference of component i across the membrane.

The separation factor β_{CO_2/H_2} was estimated as

$$\beta_{CO_2/H_2} = \frac{y_{CO_2}/y_{H_2}}{x_{CO_2}/x_{H_2}}, \tag{2}$$

where x and y in above equation represent molar fractions in the feed and permeate, respectively.

2.6. Modeling

An orthorhombic lattice was used with lattice parameters fixed at the values experimentally determined [24] at a temperature of 200 °C [a=20.11 Å, b=19.92 Å and c=13.39 Å]. The a-direction was taken to be normal to the zeolite membrane surface. Therefore, cleaved surface normals are perpendicular to the a-direction. Considering cleaved surfaces with b and c normals and choosing the planar cleaved surface to minimize the number of broken bonds, one can estimate the surface energy, using a single SiO_2 bond energy to be $444/(6.20 \times 10^{23})$ kJ $bond^{-1}$ [33], to be 1.06 J m^{-2} and 1.43 J m^{-2} for the b and c normal surfaces, respectively. We concentrated on the

b normal surface. The periodically repeated unit cell consisted of 288 atoms of silicalite-1. All calculations were performed using density functional theory (DFT) as implemented in the AIMPRO code [34,35] with the PBE exchange-correlation functional [36] and the Grimme van der Waals correction [37] (see SI, Section S2 for details).

3. Results and discussions

Graded silicalite-1 supports were prepared by co-sintering a thin layer of fine silicalite-1 particles (200 nm), that have been deposited by drop casting onto a graphite paper, onto a layer of coarse silicalite-1 particles (5 μm) by rapidly heating and subjecting the powder body to a compressive stress by pulsed current processing (PCP). It was previously shown that by identifying the material specific temperature range in combination with a compressive stress it is possible to produce strong porous supports with minimal loss of the micro-porosity of zeolite crystals by PCP [24,38–40]. The scanning electron microscope (SEM) images in Fig. 1 show that the top layer has a thickness of about 60 μm with a smooth and sharp interface without any evidence of trapping of small (200 nm) particles in the interstitial spaces between the larger zeolite crystals. The microstructure of the graded silicalite-1 membrane support (Fig. 1) is similar to commercially available alumina membrane supports (SI, Fig. 1S). BET surface area (Table 1) of the graded MFI (302 $m^2 g^{-1}$) is lower compared to the unprocessed powders (390 $m^2 g^{-1}$). The reduction in BET surface area of zeolite crystals happens during PCP-treatment due to localized sintering of zeolite crystals at the contact points [24,38–42].

Mercury intrusion porosimetry data shows that the pore size distribution of the PCP-consolidated graded silicalite-1 supports (Fig. 2, Table 1) is bimodal. The average pore size of 0.1 μm in the thin top layer of silicalite-1 substrate is sufficiently small for zeolite film growth [32] and sufficiently large to not significantly reduce the mass transport of molecules [43]. Indeed, the silicalite-1 supports show a smoother surface finish compared to commercial alumina supports (SI, Figs. 3S and 4S), which is beneficial for the formation of smooth and defect-free silicalite-1 films. The graded MFI membrane supports show reasonably high single gas permeabilities (Table 2) and a mechanical strength of 15 MPa (Table 1). The mechanical strength of the graded substrates is lower than the alumina supports but sufficiently high to sustain large pressure gradients.

Thin zeolite films were grown onto the top surface of the graded silicalite-1 supports by a combined seeding and hydrothermal synthesis route [25]. Fig. 3 shows that the calcined MFI film grown onto the graded MFI porous support was uniform, crack free and with no evidence of pinhole defects. The cross-sectional SEM image in Fig. 3a of an all-zeolite membrane shows that the MFI film has a thickness of 500 nm. Invasion of the seeding particles and growth of the zeolite film into the support pores is small and the macroporosity of the top layer of the graded support is retained.

The high resolution SEM image of the cross section (Fig. 3a) indicates that the MFI seed crystals grow in favorable orientation all the way from the substrate to the top surface of the film. Seed

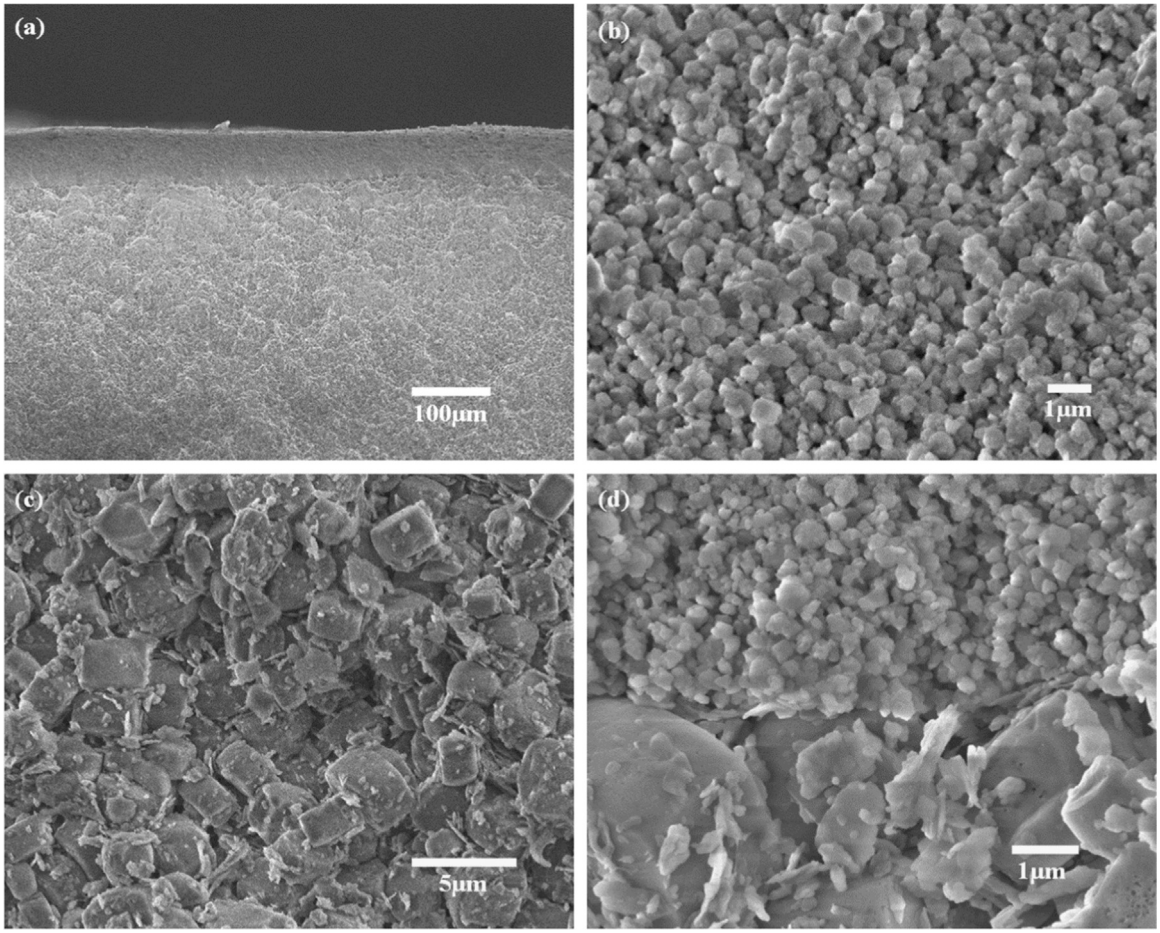

Fig. 1. SEM micrographs of PCP-consolidated graded silicalite-1 support, (a) cross-sectional view showing top and bottom layer; (b) top layer; (c) bottom layer; (d) interface between top and bottom layer.

Table 1
Properties of PCP-consolidated Silicalite-1 membrane supports.

Specimen	BET surface area[a] ($m^2\ g^{-1}$)	Total pore volume[b] ($cm^3\ g^{-1}$)	Macro-pore volume[c] ($cm^3\ g^{-1}$)	Porosity[c] (%)	Biaxial strength (MPa)	Median pore diameter [c] (μm)	Co-efficient of thermal expansion[d] (10^{-6}/°C)
Silicalite-1 powders	390	0.23	–	–	–	–	–
Graded silicalite-1 support	302	0.18	0.42	41	15	0.75, 0.1	−0.70
Alumina substrate	–	–	0.18	41	102	2.15, 0.1	8.98

[a] BET surface area ($m^2\ g^{-1}$) was calculated from nitrogen adsorption isotherms within the relative pressure range: 0.05–0.15 p/p_o.
[b] Single point adsorption total pore volume determined from nitrogen adsorption data at a relative pressure of 0.98 p/p_o.
[c] Porosity, macropore volume and median pore diameter were determined by mercury intrusion porosimetry.
[d] Determined by dilatometry in the temperature range from 200 °C to 800 °C.

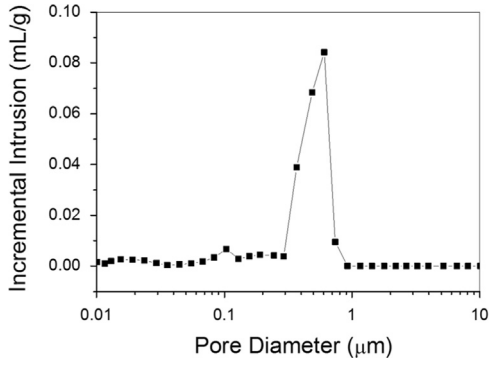

Fig. 2. Mercury intrusion porosimetry (Incremental pore volume vs mean diameter of pores) of a) PCP consolidated graded silicalite-1 membrane support.

Table 2
Single gas permeation properties of graded silicalite-1 support and all-zeolite membranes calcined at 500 °C for 6 h.

Support/ membrane	Gas	Flow [ml min^{-1}] at 0.8 bar	Permeance [10^{-7} mol s^{-1} m^{-2} Pa^{-1}]
Support	He	184	48
Support	H_2	325	86
Support	N_2	135	36
Support	CO_2	130	34
Membrane	He	177	47
Membrane	H_2	316	83
Membrane	N_2	133	35
Membrane	CO_2	130	34

crystals with no favorable orientation for growth will be encapsulated in the film. This competitive growth process corresponds well to previous observations of silicalite-1 films grown on other membrane supports [16–22]' [44]. Note that the support was masked with hydrocarbon wax during growth of the film, which prohibited growth of the zeolite crystals into the support. The single gas permeances measured for the all-zeolite membranes comprised of the thin zeolite film and the support are close to the gas permeances measured for the zeolite supports (Table 2), which shows that the mass transfer of these light molecules through the membrane is mainly limited by the support.

Fig. 4 shows the CO_2 permeance at 1 bar feed pressure for the all-zeolite membrane was 10.3×10^{-7} mol s^{-1} m^{-2} Pa^{-1}. The CO_2 permeance is somewhat lower than what is obtained for a similar membrane prepared on a graded alumina support [6], which is probably a result of higher mass transfer resistance of the zeolite support. The CO_2 permeance increases with increasing feed pressure up to 21.3×10^{-7} mol s^{-1} m^{-2} Pa^{-1} at 5 bar. The increase in the CO_2 permeance with increasing feed pressure is most likely caused by the reduced helium sweep counter-flux through the membrane at high pressure, as also reported by van de Graaf et al. [45]. In addition, the increase in the permeance may also be a result of some water being desorbed from the membrane as the feed pressure increases. In contrast, the H_2 permeance decreases from 6.0×10^{-7} mol s^{-1} m^{-2} Pa^{-1} to 1.8×10^{-7} mol s^{-1} m^{-2} Pa^{-1} when the feed pressure increases from 1 bar to 5 bar. The decrease in H_2 permeance with increasing feed pressure can be related to an increased adsorption of CO_2 in the MFI film that reduce or block the transport of H_2 through the membrane [6]. Hence, we find that the CO_2/H_2 separation factor estimated by Eq. (2) increases from 2 to 12 with increasing feed pressure. The CO_2/H_2 separation factor for the all-zeolite membranes is comparable to the separation factors achieved for previously reported MFI membranes evaluated for gas mixture separation, see Table 3.

We have calculated the surface energy of the silicalite-1 film by density functional theory. We found the relaxed surface energy of the surface perpendicular to the *a*-direction of MFI crystals after charge balancing to be 1.14 J m^{-2} (see SI, Section S2). We note that the calculated value is significantly higher than the commonly quoted value of 0.1 J m^{-2} for silica surfaces [51].

The CTE of the graded silicalite-1 support ($\alpha_{silicalite\text{-}1} = -0.7 \times 10^{-6}\ °C^{-1}$) and the alumina support ($\alpha_{Al_2O_3} = +8.98 \times 10^{-6}\ °C^{-1}$) was determined by dilatometer and is reported in Table 1. The CTE of a silicalite-1 film ($\alpha_f = -2.00 \times 10^{-6}\ °C^{-1}$) was taken from the literature [23]. We adopted the laminate model of stress relaxation from our previous work [24] to predict the critical film thickness of silicalite-1 to avoid cracking in a thermal cycling process. The model assumes that cracks appear in the thin film when the stored energy exceeds the surface energy of the film material. We used the DFT-based estimate of surface energy (1.14 J m^{-2}) of silicalite-1, a Poison's ratio of 0.175, and an elastic modulus of 40×10^9 Pa [52,53] together with CTE of silicalite-1 film ($\alpha_f = -2.00 \times 10^{-6}\ °C^{-1}$) [23] and measured CTE of the graded silicalite-1 substrate ($\alpha_{silicalite\text{-}1} = -0.7 \times 10^{-6}\ °C^{-1}$) and alumina substrate ($\alpha\alpha_{Al_2O_3} = +8.98 \times 10^{-6}\ °C^{-1}$) to estimate the critical film thickness.

Fig. 5 shows that all-zeolite membranes with zeolite films as thick as 5 μm can sustain temperature differences as high as 800 °C without cracking, while the critical film thickness of a silicalite-1 film onto an alumina substrate is around 500 nm at a moderate ΔT of 400 degrees, which is lower temperature cycle limit for most zeolite membranes [54]. Hence, while our estimates suggest that typical calcination processes at 400–600 °C may be sufficient to produce defects such as crack and open grain boundaries in alumina-supported zeolite films, all-zeolite membranes may provide defect free membranes that not only can avoid defect formation during the critical calcination step at 400–600 °C but also sustain high temperature thermal cycling.

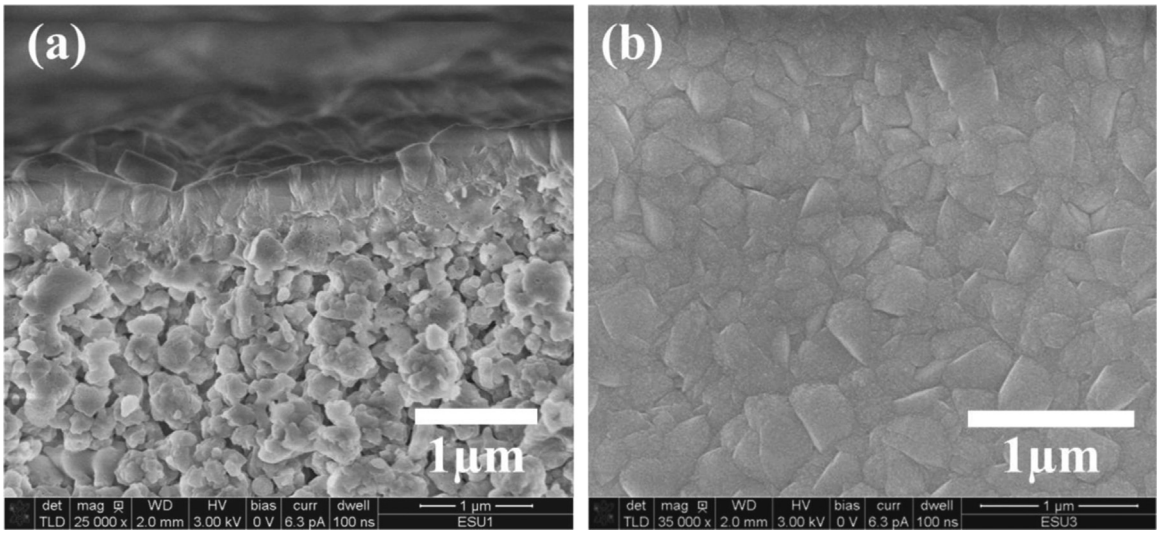

Fig. 3. SEM micrographs of all-zeolite membrane, (a) cross section and (b) top view (see SI, Fig. 5S for magnified images).

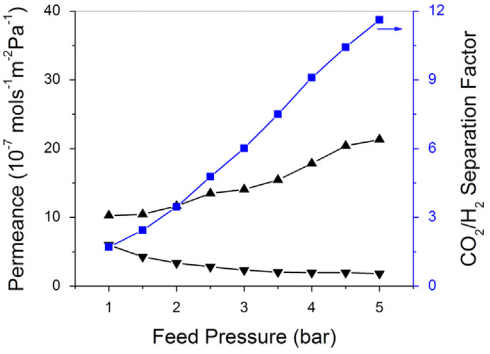

Fig. 4. Permeances of CO_2 and H_2 as a function of feed pressure at 0 °C. ▲—CO_2 permeance, ▼—H_2 permeance, and CO_2/H_2 separation factor as a function of feed pressure.

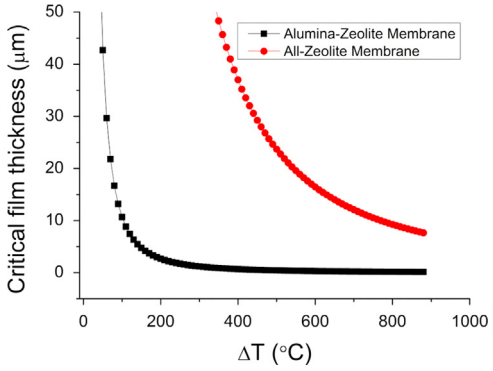

Fig. 5. A comparison of critical film thickness to avoid thermal cracking during thermal cycling of temperature difference (ΔT) between alumina-supported zeolite membrane and all-zeolite membrane.

Table 3
Summary of studies on CO_2 separation from H_2 gas using MFI membranes prepared on non-zeolite supports.

Feed mixture	Feed pressure (bar)	Temp. (°C)	CO_2 permeance (10^{-7} mol m^{-2} s^{-1} Pa^{-1})	CO_2/H_2 separation factor	Ref.
CO_2/H_2	1	0	10.3	2	This work
CO_2/H_2	5	0	21.3	12	This work
CO_2/H_2	1	22	3.8	12	[46]
CO_2/H_2	1	20	7	17	[47]
CO_2/H_2	3.3	25	1.2	10	[48]
CO_2/H_2	1	25	12	3.4	[49]
CO_2/H_2	1	22	13	2.2	[49]
CO_2/H_2[a]	1	25	11.7	6.2	[50]
CO_2/H_2	10	23	93	15	[6]

[a] Saturated with water at 20 °C.

4. Conclusions

All-zeolite membranes were prepared to minimize the thermal expansion mismatch between the graded support and the zeolite film to minimize crack formation during calcination and thermal cycling. We prepared graded silicalite-1 supports with a tailored porous architecture with good permeability and low surface roughness suitable for silicalite-1 film growth by a modified pulsed current powder processing route. Thin (500 nm) silicalite-1 films were grown on the graded zeolite supports using a previously develop route based on masking and seeded hydrothermal growth. The resulting all-zeolite membranes showed a high permeance and CO_2/H_2 separation selectivity. Estimates of thermal cracking based on calculated surface energies and measured thermal expansion coefficients of the support show that all-zeolite membranes could remain crack-free during the critical calcination step and can undergo thermal cycling from temperatures exceeding 500 °C to room temperature without cracking. Tailoring the properties of all-zeolite membranes could extend the application of zeolite membranes in demanding separation processes involving with high temperature thermal cycling. The method of preparing zeolite membrane supports is generic and can be implemented to produce other framework types of all-zeolite and possibly also all-metal organic framework membranes.

Acknowledgements

The Swedish Foundation for Strategic Research is gratefully acknowledged for financially supporting this work. M. Rayson thanks the Swedish Research Council (VR) for financial support for the project 2012-3174. F. Akhtar acknowledges Christina Schütz for AFM measurements, Segey Istomin and Gunnar Svensson for thermal expansion measurements, Damian Hodel and Sajid Alvi for experimental assistance in developing silicalite-1 membrane supports.

Appendix A. Supplementary information

Supplementary data associated with this article can be found in the online version at http://dx.doi.org/10.1016/j.memsci.2015.06.020.

References

[1] E.E. McLeary, J.C. Jansen, F. Kapteijn, Zeolite based films, membranes and membrane reactors: progress and prospects, Microporous Mesoporous Mater. 90 (2006) 198–220.
[2] A.S.T. Chiang, K. Chao, Membranes and films of zeolite and zeolite-like materials, J. Phys. Chem. Solids 62 (2001) 1899–1910.
[3] J. Caro, M. Noack, P. Kölsch, R. Schäfer, Zeolite membranes—state of their development and perspective, Microporous Mesoporous Mater. 38 (2000) 3–24.
[4] T.C. Bowen, R.D. Noble, J.L. Falconer, Fundamentals and applications of pervaporation through zeolite membranes,, J. Membr. Sci. 245 (2004) 1–33.
[5] Z. Wang, Q. Ge, J. Shao, Y. Yan, High performance zeolite LTA pervaporation membranes on ceramic hollow fibers by dipcoating – wiping seed deposition, J. Am. Chem. Soc. 131 (2009) 6910–6911.
[6] L. Sandström, E. Sjöberg, J. Hedlund, Very high flux MFI membrane for CO_2 separation, J. Membr. Sci. 380 (2011) 232–240.
[7] M. Zhou, D. Korelskiy, P. Ye, M. Grahn, J. Hedlund, A uniformly oriented MFI membrane for improved CO_2 separation, Angew. Chem. Int. Ed. 53 (2014) 3492–3495.
[8] J. Caro, M. Noack, Zeolite membranes—recent developments and progress, Microporous Mesoporous Mater. 115 (2008) 215–233.
[9] J.C. Aisheng Huang, F. Liang, F. Steinbach, T.M. Gesing, Neutral and cation-free LTA-type aluminophosphate ($AlPO_4$) molecular sieve membrane with high hydrogen permselectivity, J. Am. Chem. Soc. 132 (2010) 2140–2141.
[10] S.S. Himeno, T. Tomita, K. Suzuki, K. Nakayama, K. Yajima, Yoshida, Synthesis and permeation properties of a DDR-type zeolite membrane for separation of CO_2/CH_4 gaseous mixtures, Ind. Eng. Chem. Res. (2007) 6989–6997.
[11] A. Huang, F. Liang, F. Steinbach, T.M. Gesing, J. Caro, Neutral and cation-free LTA-type aluminophosphate ($AlPO_4$) molecular sieve membrane with high hydrogen permselectivity, J. Am. Chem. Soc. 132 (2010) 2140–2141.
[12] A. Navajas, R. Mallada, C. Téllez, J. Coronas, M. Menéndez, J. Santamaría, Preparation of mordenite membranes for pervaporation of water-ethanol mixtures, Desalination 148 (2002) 25–29.
[13] M. Matsukata, K. Sawamura, T. Shirai, M. Takada, Y. Sekine, E. Kikuchi, Controlled growth for synthesizing a compact mordenite membrane, J. Membr. Sci. 316 (2008) 18–27.
[14] J. Choi, H.K. Jeong, M.A. Snyder, J.A. Stoeger, R.I. Masel, M. Tsapatsis, Grain boundary defect elimination in a zeolite membrane by rapid thermal processing, Science 325 (2009) 590–593.
[15] M. Tsapatsis, Toward high-throughput zeolite membranes, Science 334 (2011) 767–768.
[16] T. Bein, Synthesis and applications of molecular sieve layers and membranes, Chem. Mater. 8 (1996) 1636–1653.
[17] M.R. Othman, S.C. Tan, S. Bhatia, Separability of carbon dioxide from methane using MFI zeolite-silica film deposited on gamma-alumina support, Microporous Mesoporous Mater. 121 (2009) 138–144.
[18] F. López, M.P. Bernal, R. Mallada, J. Coronas, J. Santamaría, Preparation of silicalite membranes on stainless steel grid supports, Ind. Eng. Chem. Res. 44 (2005) 7627–7632.
[19] T. Mohammadi, A. Pak, Effect of calcination temperature of kaolin as a support for zeolite membranes, Sep. Purif. Technol. 30 (2003) 241–249.
[20] M.A. Ulla, R. Mallada, J. Coronas, L. Gutierrez, E. Miró, J. Santamaría, Synthesis and characterization of ZSM-5 coatings onto cordierite honeycomb supports, Appl. Catal., A Gen. 253 (2003) 257–269.
[21] W.-Y. Dong, Y.-C. Long, Preparation of an MFI-type zeolite membrane on a porous glass disc by substrate self-transformation, Chem. Commun. (2000) 1067–1068.
[22] Á. Berenguer-Murcia, J. García-Martínez, D. Cazorla-Amorós, Á. Linares-Solano, A.B. Fuertes, Silicalite-1 membranes supported on porous carbon discs, Microporous Mesoporous Mater. 59 (2003) 147–159.
[23] H.-K. Jeong, Z. Lai, M. Tsapatsis, J.C. Hanson, Strain of MFI crystals in membranes: an in situ synchrotron X-ray study, Microporous Mesoporous Mater. 84 (2005) 332–337.
[24] F. Akhtar, A. Ojuva, S.K. Wirawan, J. Hedlund, L. Bergström, Hierarchically porous binder-free silicalite-1 discs: a novel support for all-zeolite membranes, J. Mater. Chem. 21 (2011) 8822.
[25] J. Hedlund, J. Sterte, M. Anthonis, A.-J. Bons, B. Carstensen, N. Corcoran, et al., High-flux MFI membranes, Microporous Mesoporous Mater. 52 (2002) 179–189.
[26] S. Miachon, P. Ciavarella, L. van Dyk, I. Kumakiri, K. Fiaty, Y. Schuurman, et al., Nanocomposite MFI-alumina membranes via pore-plugging synthesis: specific transport and separation properties, J. Membr. Sci. 298 (2007) 71–79.
[27] Y. Yushan, M.E. Davis, G.R. Gavalas, Preparation of highly selective zeolite ZSM-5 membranes by a post-synthetic coking treatment, J. Membr. Sci. 123 (1997) 95–103.
[28] M. Nomura, T. Yamaguchi, S.-I. Nakao, Silicalite membranes modified by counterdiffusion CVD technique, Ind. Eng. Chem. Res. 36 (1997) 4217–4223.
[29] M.D. Thouless, Modeling the development and relaxation of stresses in films, Annu. Rev. Mater. Sci. 25 (1995) 69–96.
[30] M.D. Thouless, Crack spacing in brittle films on elastic substrates, J. Am. Ceram. Soc. 73 (1990) 2144–2146.
[31] F. Akhtar, L. Andersson, N. Keshavarzi, L. Bergström, Colloidal processing and CO_2 capture performance of sacrificially templated zeolite monoliths,, Appl. Energy 97 (2012) 289–296.
[32] J. Hedlund, F. Jareman, A.-J. Bons, M. Anthonis, A masking technique for high quality MFI membranes, J. Membr. Sci. 222 (2003) 163–179.
[33] Y.K. Shchipalov, Surface energy of crystalline and vitreous silica, Glass Ceram. (English Transl. Steklo I Keramika) 57 (2000) 374–377.
[34] M.J. Rayson, P.R. Briddon, Highly efficient method for Kohn-Sham density functional calculations of 500-10000 atom systems, Phys. Rev. B—Condens. Matter Mater. Phys. 80 (2009).
[35] M.J. Rayson, P.R. Briddon, Rapid iterative method for electronic-structure eigenproblems using localised basis functions, Comput. Phys. Commun. 178 (2008) 128–134.
[36] J.P. Perdew, K. Burke, M. Ernzerhof, Generalized gradient approximation made simple, Phys. Rev. Lett. 77 (1996) 3865–3868.
[37] S. Grimme, Semiempirical GGA-type density functional constructed with a long-range dispersion correction, J. Comput. Chem. 27 (2006) 1787–1799.
[38] F. Akhtar, L. Andersson, S. Ogunwumi, N. Hedin, L. Bergström, Structuring adsorbents and catalysts by processing of porous powders, J. Eur. Ceram. Soc. (2014).
[39] F. Akhtar, Q. Liu, N. Hedin, L. Bergström, Strong and binder free structured zeolite sorbents with very high CO_2-over-N_2 selectivities and high capacities to adsorb CO_2 rapidly, Energy Environ. Sci. 5 (2012) 7664.
[40] P. Vasiliev, F. Akhtar, J. Grins, J. Mouzon, C. Andersson, J. Hedlund, et al., Strong hierarchically porous monoliths by pulsed current processing of zeolite powder assemblies, ACS Appl. Mater. Interfaces 2 (2010) 732–737.
[41] F. Akhtar, N. Keshavarzi, D. Shakarova, O. Cheung, N. Hedin, L. Bergström, Aluminophophate monoliths with high CO_2-over-N_2 selectivity and CO_2 capture capacity, RSC Adv. 4 (99) (2015) 55877–55883.
[42] F. Akhtar, L. Bergström, Colloidal procesing and thermal treatment of binderless hierarchically porous zeolite 13X monoliths for CO_2 capture, J. Am. Ceram. Soc. 94 (2011) 92–98.
[43] S.K. Wirawan, D. Creaser, J. Lindmark, J. Hedlund, I.M. Bendiyasa, W. B. Sediawan, H_2/CO_2 permeation through a silicalite-1 composite membrane, J. Membr. Sci. 375 (2011) 313–322.
[44] J. Hedlund, F. Jareman, Texture of MFI films grown from seeds, Curr. Opin. Colloid Interface Sci. 10 (2005) 226–232.
[45] J.M. Van De Graaf, F. Kapteijn, J.a. Moulijn, Methodological and operational aspects of permeation measurements on silicalite-1 membranes, J. Membr. Sci. 144 (1998) 87–104.
[46] W.J.W. Bakker, F. Kapteijn, J. Poppe, J.A. Moulijn, Permeation characteristics of a metal-supported silicalite-1 zeolite membrane, J. Membr. Sci. 117 (1996) 57–78.
[47] H. Guo, G. Zhu, H. Li, X. Zou, X. Yin, W. Yang, et al., Hierarchical growth of large-scale ordered zeolite silicalite-1 membranes with high permeability and selectivity for recycling CO_2, Angew. Chem. Int. Ed. 45 (2006) 7053–7056.
[48] A. Alshebani, M. Pera-Titus, E. Landrivon, T. Schiestel, S. Miachon, J.-A. Dalmon, Nanocomposite MFI—ceramic hollow fibres: prospects for CO_2 separation, Microporous Mesoporous Mater. 115 (2008) 197–205.
[49] J. Lindmark, J. Hedlund, Modification of MFI membranes with amine groups for enhanced CO_2 selectivity, J. Mater. Chem. 20 (2010) 2219–2225.
[50] J. Lindmark, J. Hedlund, Carbon dioxide removal from synthesis gas using MFI membranes, J. Membr. Sci. 360 (2010) 284–291.
[51] A. Navrotsky, Energetics of nanoparticle oxides: interplay between surface energy and polymorphism, Geochem. Trans. 4 (2003) 34–37.
[52] Z.B. Wang, A. Mitra, H.T. Wang, L.M. Huang, Y. Yan, Pure silica zeolite films as low-k dielectrics by spin-on of nanoparticle suspensions, Adv. Mater. 13 (2001) 1463–1466.
[53] M.C. Johnson, J. Wang, Z. Li, C.M. Lew, Y. Yan, Effect of calcination and polycrystallinity on mechanical properties of nanoporous MFI zeolites, Mater. Sci. Eng., A 456 (2007) 58–63.
[54] Z. Wang, Y. Yan, Controlling crystal orientation in zeolite MFI thin films by direct in situ crystallization, Chem. Mater. 13 (2001) 1101–1107.